# $^{55}$Mn nuclear magnetic resonance study of highly Sr-doped $La_{2-2x}Sr_{1+2x}Mn_2O_7$ ($x=0.5-0.8$)

D. Rybicki,[1,2] Cz. Kapusta,[1] W. Tokarz,[1] H. Štěpánková,[3] V. Procházka,[3] J. Haase,[2] Z. Jirák,[4] D. T. Adroja,[5] and J. F. Mitchell[6]
[1]*Department of Solid State Physics, Faculty of Physics and Applied Computer Sciences, AGH-University of Science and Technology, Al. Mickiewicza 30, 30-059 Krakow, Poland*
[2]*Faculty of Physics and Earth Science, Leipzig University, Linnéstraße 5, 04103 Leipzig, Germany*
[3]*Department of Low Temperature Physics, Faculty of Mathematics and Physics, Charles University in Prague, V. Holešovičkách 2, 180 00 Prague 8, Czech Republic*
[4]*Institute of Physics, Cukrovarnická 10, 162 53 Prague 6, Czech Republic*
[5]*ISIS Facility, Rutherford Appleton Laboratory, Chilton, Didcot OX11 0QX, United Kingdom*
[6]*Center for Nanoscale Materials, Materials Science Division, Argonne National Laboratory, 9700 South Cass Avenue, Argonne, Illinois 60439, USA*

(Received 13 May 2008; revised manuscript received 13 September 2008; published 20 November 2008)

The $^{55}$Mn nuclear magnetic resonance (NMR) study of bilayered perovskites $La_{2-2x}Sr_{1+2x}Mn_2O_7$ with $0.5 \leq x \leq 1$ is presented. The $^{55}$Mn spin-echo spectra were measured at 4.2 K at zero applied magnetic field and at fields up to 2.5 T. Recent neutron-diffraction studies report that all the compounds studied are antiferromagnetically ordered (except $x=0.68$ in which no long-range magnetic order was found) [Mitchell *et al.*, J. Phys. Chem. B **105**, 10731 (2001)]. However, within the doping range $0.62 \leq x \leq 0.68$, apart from NMR signal from antiferromagnetic insulating (AFI) phase, also lines from ferromagnetic insulating (FMI) and ferromagnetic metallic (FMM) phases are observed. This indicates that phase separation occurs in high Sr-doped bilayered manganites. The amount of the FMI and FMM regions decreases with the Sr doping level and for compounds with $x=0.75$ and $x=0.8$; only the line originating from nuclei in $Mn^{4+}$ cations in AFI regions is observed.

DOI: 10.1103/PhysRevB.78.184428 PACS number(s): 75.47.Lx, 75.47.Gk, 76.60.−k

## I. INTRODUCTION

Bilayered manganese perovskites belong to a broader family of so-called Ruddlesden-Popper phases, which are described by general formula $(A,B)_{n+1}Mn_nO_{3n+1}$, where $A$ and $B$ are trivalent and divalent cations, respectively. These systems include both the pseudocubic perovskites ($n=\infty$) and systems based on single ($n=1$) or multiple perovskite layers. The most common examples of the bilayered perovskites ($n=2$) are the mixed valent ($Mn^{3+}/Mn^{4+}$) compounds $La_{2-2x}Sr_{1+2x}Mn_2O_7$, where $x$ gives the actual $Mn^{4+}$ content.

Manganese perovskites are of considerable research interest associated mainly with the colossal magnetoresistance, which they exhibit near the ferromagnetic ordering temperature. Such close interrelation of the magnetic and electronic properties arises due to fact that the electrons responsible for magnetic moments and for conduction are of the same $3d$ kind. The interplay of lattice, charge, spin, and orbital degrees of freedom results in very rich phase diagrams[1–5] and a variety of electronic and magnetic properties ranging from a metallic or insulating ferromagnetic (FM) to antiferromagnetic (AF) insulating (AFI) or paramagnetic insulating behavior. Such a behavior arises from a strong competition between double exchange (DE),[6,7] superexchange, and electron-phonon interactions.

The coexistence of various magnetic and electronic phases was found in manganese perovskites by means of many different techniques such as transmission electron microscopy,[8] scanning tunneling microscopy,[9] and electron holography. Further in Ref. 8 the authors found the phase exhibiting simultaneously charge ordering and ferromagnetic properties, which were previously believed to be mutually exclusive.[10] The effect of the applied magnetic field on the coexisting paramagnetic and FM phases was presented by Yoo *et al.*[11] Phase separation picture also attracted interest of theorists who proposed models explaining some of the phenomena observed in manganese perovskites.[12–17]

The compounds of interest, $La_{2-2x}Sr_{1+2x}Mn_2O_7$ ($0.5 \leq x \leq 1$) have a crystal lattice consisting of bilayers of $MnO_6$ octahedra separated by $(La,Sr)_2O_2$ layers, which results in a reduced dimensionality and highly anisotropic properties.[18,19] This offers a unique possibility to compare the results with three-dimensional pseudocubic perovskites. The compounds studied also exhibit different types of the magnetic ordering as a function of Sr doping, $x$, which are presented in Fig. 1, after Ref. 1. The $x=0.5$ compound is an $A$-type AF, i.e., magnetic moments in a single layer (within the plane perpendicular to lattice $c$ axis) are FM coupled, but the coupling between two layers is AF. This type of ordering was suggested up to Sr doping of $x=0.66$.[1] Very interesting region was found to exist in the doping range $0.66 \leq x < 0.74$, where the neutron powder diffraction showed no magnetic long-range order (LRO).[20] Up to $x=0.74$ the crystal structure is tetragonal ($I4/mmm$). Within the doping range $0.75 \leq x < 0.92$ the crystal structure at low temperatures belongs to orthorhombic $Immm$ space group. The neutron powder diffraction revealed two AF superstructures, referred as type $C$ and type $C^*$, in which the lattice parameter $c$ is doubled.[20] Above $x=0.92$ a $G$-type magnetic order was found.[21] The ideal $G$-type magnetic order, found for $x=1$, involves all nearest Mn-Mn neighbors coupled AF, with their spins aligned parallel to the $c$ axis. Below $x=1$ spins tilt from the $c$ axis toward plane perpendicular to it.[20] Therefore, according to Goodenough's theoretical predictions, when increasing $Mn^{4+}$ content (increasing number of holes in the $e_g$ orbital) one successively obtains "less ferromagnetism" (sheets-to-rods-to-points).[1]

 

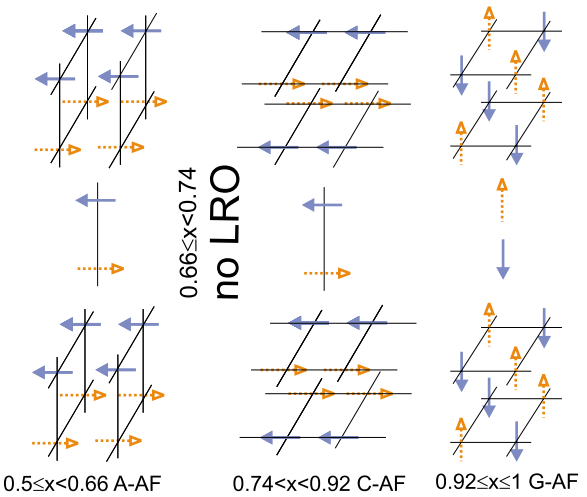


FIG. 1. (Color online) Magnetic ordering types of $La_{2-2x}Sr_{1+2x}Mn_2O_7$ series of compounds at 5 K, determined by the neutron powder diffraction, after Ref. 1.

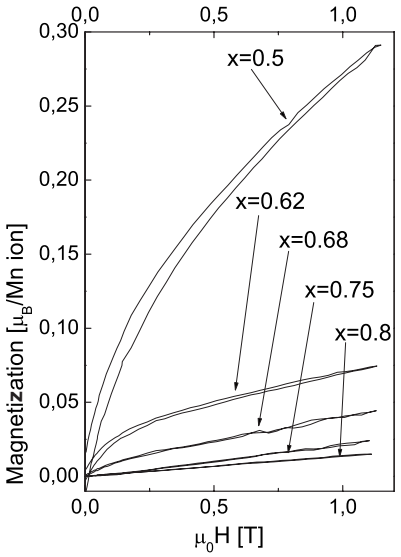


FIG. 2. Magnetization versus applied field, $M(H)$, curves measured at 4.2 K for all the compounds studied.

Spectroscopic methods such as electronic spin resonance (ESR) and nuclear magnetic resonance (NMR) can provide information on magnetic and electronic properties on the microscopic scale and, therefore, are very suitable to study the phase segregation which occurs in mixed valence manganites. The ESR study of the phase-separated Ca-doped pseudocubic perovskites was recently presented in Ref. 22. First NMR results on manganese perovskites were presented in Refs. 23–28. Phase separation observed with the NMR method manifests itself with distinct resonant lines in the frequency-swept NMR spectrum, which are ascribed to the respective magnetic (ferromagnetic or antiferromagnetic) and electronic (insulating or metallic) phases.

It is worth mentioning that $^{55}$Mn NMR experiments for lower Sr-doped bilayered manganites (i.e., $x<0.5$) have already been reported and the results also indicated existence of the phase separation.[29,30] NMR is a powerful tool in studying magnetic and electronic properties of the distinct atomic or ionic sites in the magnetically ordered systems. The resonant response of nuclear magnetic moments at individual sites provides information on the local magnetic states. The resonance condition is $2\pi\upsilon = \gamma B_{\mathrm{loc}}$, where $\gamma$ is the gyromagnetic ratio, which for $^{55}$Mn nuclei amounts to 10.55 MHz/T, and $B_{\mathrm{loc}}$ is the local magnetic field at nucleus. This field in the magnetically ordered state is mostly of the hyperfine origin and is synonymously termed the hyperfine field, $B_{\mathrm{HF}}$. The formula for the local field related to the spins of the parent atom/ion and its neighbors can be written in the following way:

$$\vec{B}^i_{\mathrm{loc}} = \frac{2\pi}{\gamma} g\mu_B \left( \tilde{A}^i \langle \tilde{S}^i \rangle + \sum_j B^j \langle \vec{S}^j \rangle \right) + \vec{B}_0, \qquad (1)$$

where $\langle \vec{S}^i \rangle$ and $\langle \vec{S}^j \rangle$ are on-site and nearest-neighbor electron spins, $\tilde{A}^i$ and $B^j$ are the respective hyperfine couplings ($\tilde{A}^i$ is a tensor and $B^j$ is of scalar nature), and $\vec{B}_0$ is the external field.[23] The magnitude of the local field, $B_{\mathrm{loc}}$, and the corresponding resonant frequency in the case of manganese perovskites were found to be lower for the antiferromagnetic neighborhood.[23,28] This is because the sign of the "transferred" $B_{\mathrm{HF}}$, which is represented by the second term in parenthesis, depends on the orientation of neighboring spins; therefore, the transferred field from the AF coupled neighbors is of opposite sign compared with that in the FM neighborhood.

## II. EXPERIMENT

Polycrystalline samples of $La_{2-2x}Sr_{1+2x}Mn_2O_7$ ($0.5 \leq x \leq 1$) studied were prepared by the high-temperature solid-state reaction method, which is thoroughly described in Ref. 31.

The samples were characterized by magnetization ($M$) versus field ($H$) measurements (Fig. 2) carried out using the vibrating sample magnetometer. $M$ versus $H$ curves of compounds with $x=0.5$, $x=0.62$, and $x=0.68$ show a ferromagneticlike component although these compounds are reported in literature to be AF ($x=0.5$ and $x=0.62$) or to have no LRO ($x=0.68$). One can notice that magnetization at the highest field measured decreases with increasing Sr doping, which could be due to decrease in the "nominal" average magnetic moment of Mn with doping (in the case of FM order the "nominal" Mn magnetic moment decreases from $3.5\mu_B$ to $3.2\mu_B$ for $x=0.5$ and $x=0.8$ compounds, respectively). However, the main reason of magnetization decrease is "strengthening" of antiferromagnetism with Sr doping. The FM component quickly decreases with increasing doping, and the $M$ versus $H$ curves for compounds with $x=0.7$ and $x=0.8$ are straight lines as expected for ideal AF.

The $^{55}$Mn NMR experiments were carried out using a frequency-swept spin-echo spectrometer (Bruker Avance) with an untuned probe coil. Measurements were performed at 4.2 K and in static magnetic fields of 0, 1, 2, or 2.5 T using a superconducting solenoid magnet. A sequence of two radio-frequency (rf) pulses, $t-\tau-2t$, was used (with a typical

pulse spacing $\tau$ of 12 $\mu$s) and the spin-echo signal was averaged and then integrated.

For optimal excitation of the NMR spin-echo signal (i.e., to obtain maximal signal at a given frequency) the first rf pulse should be adjusted to turn the nuclear magnetization from its equilibrium by an angle $\pi/2$. The condition for the $\pi/2$ pulse depends in fact on the product of the pulse duration $t$ and the rf field amplitude. Therefore, the dependences of the spin-echo signal on the rf pulse duration were measured (at a fixed rf amplitude) for all of the resonance lines observed in the frequency-swept spectrum, starting from short pulses of 0.1 $\mu$s up to 8 $\mu$s, in order to find the first maximum of the spin-echo signal. Alternatively, dependences of the spin-echo signal at a given frequency on the rf field amplitude with fixed length of pulses were measured.

In magnetic materials a well-known effect of the rf field enhancement occurs.[32] The reason is that the quantum resonant transitions of nuclear spins are induced not only directly by the applied $B_{\mathrm{rf}}$, but also by the alternating (oscillating) transversal part $B_{\mathrm{loc}}^{\perp}$ of the local field $B_{\mathrm{loc}}$ acting on the nuclei. Oscillations of $B_{\mathrm{loc}}$ are induced via strong hyperfine coupling by oscillations of atomic (ionic) magnetic moments in the applied $B_{\mathrm{rf}}$. In summary, when an external radio frequency field of intensity $B_{\mathrm{rf}}$ is applied to a magnetic sample, the nuclei feel an additional enhanced field $B_{\mathrm{loc}}^{\perp}=\eta B_{\mathrm{rf}}$, where $\eta$ is the NMR enhancement factor.

Mechanisms of rf field enhancement are different in the case of antiferromagnet or ferromagnet. Additionally in ferromagnet enhancement mechanism is also different for nuclei in domains from that in domain walls. Consequently $\eta$ has different values for nuclei in antiferromagnet (the smallest values of $\eta$, $\eta<20$), nuclei in domains in ferromagnet ($\eta$ up to 100), and in domain walls in ferromagnet ($\eta$ even larger than $10^4$). In principle, knowing $\eta$ of different NMR signals it is possible to distinguish whether the signal comes from ferromagnetic or antiferromagnetic regions.

Taking into account the enhancement of rf field in magnetics, the parameters of the $\pi/2$ pulse are given by equation

$$\gamma\eta B_{\mathrm{rf}}t=\pi/2, \tag{2}$$

so that the determination of differences in the values of $B_{\mathrm{rf}}t$ at optimal excitation of particular lines yields the possibility to compare the corresponding enhancement factors $\eta$ with the aim to identify their origin.

Analogous processes enhance the NMR signals created by Larmor precession of the nuclear magnetization; thus, the intensities of the signals detected by a NMR coil are also amplified.[23] Therefore, to obtain information about relative amount of nuclei that contribute to particular lines in a spectrum one has to consider besides the line intensities also the differences in their enhancement factors.

### A. NMR spectra of $La_{2-2x}Sr_{1+2x}Mn_2O_7$, $x=0.5$, 0.62, and 0.68

Figure 3 presents the $^{55}$Mn NMR spin-echo spectra of $La_{2-2x}Sr_{1+2x}Mn_2O_7$ for $x=0.5$, $x=0.62$, and $x=0.68$ compounds measured at 4.2 K and zero applied field, with intensity correction for different enhancement factors of individual lines. Due to very different values of $\eta$ and line

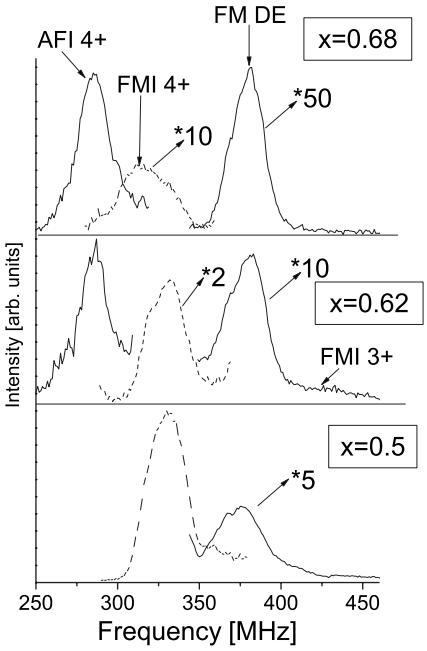


FIG. 3. $^{55}$Mn NMR spin-echo spectra of $La_{2-2x}Sr_{1+2x}Mn_2O_7$ for $x=0.5$, $x=0.62$, and $x=0.68$ at 4.2 K and zero applied field. Abbreviations denote AFI 4+ ($Mn^{4+}$ ions in antiferromagnetic insulating regions), FMI 4+ ($Mn^{4+}$ ions in ferromagnetic insulating regions), FMI 3+ ($Mn^{3+}$ ions in ferromagnetic insulating regions), and FM DE ($Mn^{3+/4+}$ ions in the double exchange controlled ferromagnetic metallic regions). Different values of NMR signal enhancement appear due to differences in NMR enhancement factors $\eta$ of particular lines; therefore, corrections of line intensities due to enhancement effects were applied where the lower limit of the enhancement for the FM lines with respect to the AF lines was considered (see the text).

overlap they were measured at excitation conditions optimal for particular line [ferromagnetic insulating (FMI) and ferromagnetic metallic (FMM) lines] or at maximal available excitation angle (for the AFI line, when conditions of $\pi/2$ pulse were not obtained even with maximal rf power) and they are presented separately. The dashed line corresponds to measurements at conditions optimal for FMI line at 325 MHz.

For the $x=0.5$ Sr-doped compound there are several lines observed (Fig. 3) at 329 MHz (31.2T), 376 MHz (35.6 T), and above 400 MHz, i.e., lines denoted as FMI 4+, FM DE, and FMI 3+, respectively. The line at the lowest frequency (329 MHz) is attributed to $Mn^{4+}$ ions in the FMI phase[33] and signals above 400 MHz are attributed to $Mn^{3+}$ ions also in FMI phase. The line at about 375 MHz (between signals from $Mn^{4+}$ and $Mn^{3+}$ ions in FMI phases) is assigned to Mn ions with the valence averaged (between 3+ and 4+) due to the DE interaction.[33] Observation of this line indicates that the characteristic time of the electron hopping due to the DE interaction is much shorter than the difference between the Larmor precession periods of the nuclear magnetic moments in the two states (3+ and 4+) when the direction of the $B_{\mathrm{HF}}$ does not change, i.e., $\ll 5\times10^{-9}$ s. Therefore this resonant line is attributed to the Mn ions in the DE-controlled FMM regions.[33] The amount of the FMM phase is much smaller than that of the FMI phase.

For the $x=0.62$ compound the $Mn^{4+}$ line from FMI regions at 330 MHz, the DE line at 378 MHz, and weak signals from $Mn^{3+}$ ions in FMI regions above 400 MHz are also detected. However, an additional line centered at 284 MHz is observed. In the literature reporting $^{55}$Mn NMR results on manganese perovskites the lines below 300 MHz are ascribed to the $Mn^{4+}$ ions in AFI regions.[23,27,34]

The distinction, which line is due to AF or FM order, can be proven by carrying out measurements in the applied magnetic field $B_0$. If manganese moments are coupled FM and the external field is higher than the demagnetization field, the resonant frequency shifts toward lower frequencies (i.e., $B_{loc}$ decreases). This is due to the fact that the $B_{HF}$ is the dominant contribution to $B_{loc}$ and is antiparallel to the manganese electronic magnetic moment. The biggest contribution to the $B_{HF}$ comes from the Fermi contact field, $B_{Fermi}$, which results from the contact interaction of the nuclear magnetic moment with the *s*-like electrons, polarized mostly by the *d*-like electronic magnetic moments.[35] This field is antiparallel to the electronic magnetic moment and, consequently, $B_{HF}$ and $B_{loc}$ are also antiparallel to the electronic magnetic moment.

In an antiferromagnet with low magnetocrystalline anisotropy or with easy magnetization direction of the easy-plane type, as expected for the compounds studied, the sublattice magnetizations will tend to align perpendicularly to the applied field. This is because the perpendicular susceptibility is larger than the parallel one. Hence, the resonant frequency corresponding to $B_{loc}$, which is a vector sum of $B_{HF}$ and a much smaller $B_0$, changes only a little compared to that in zero applied field.[23] In such a situation the AF line only broadens without noticeable shift in frequency.[36] Comparing the relative intensities of all the observed lines for compounds with $x=0.5$, 0.62, and 0.68 (Fig. 3), it is clear that the intensity of the $Mn^{4+}$ FMI line decreases with respect to the FM DE line at the expense of the $Mn^{4+}$ AFI line. This indicates that the amount of the AFI phase is increasing with doping, which agrees with the magnetization measurements. The intensity of the FMI line may seem to be big compared with the AFI line corresponding to the majority phase. However, we were unable to provide optimal excitation conditions for AFI lines; i.e., with the highest rf power available and the longest pulses we still could not reach them. This caused an underestimation of the intensities of the AFI lines.

One has to mention that in lower Sr-doped compounds ($x \leq 0.5$) a small amount of intergrowths was found both in single crystals[37] and in polycrystalline samples.[38] Intergrowths were identified to be FM ordered,[37] and therefore, it cannot be excluded that FMI or FMM signals can be partly due to intergrowths. However, to our knowledge there are no studies of this problem in Sr doping range discussed in the article.

Figure 4 presents the NMR measurements of $La_{0.76}Sr_{2.24}Mn_2O_7$ ($x=0.62$) compound at 0, 1, and 1.5 T at 4.2 K (not corrected for differences in $\eta$). As expected for the signal from the AF ordered magnetic moments the line at 284 MHz does not change its position significantly in the applied field, in contrast to the DE line (at 378 MHz), which shifts toward lower frequencies as is characteristic for the FM ordered moments. The resonant frequency of the DE line shifts to 367 MHz at 1 T, which agrees well with the value of

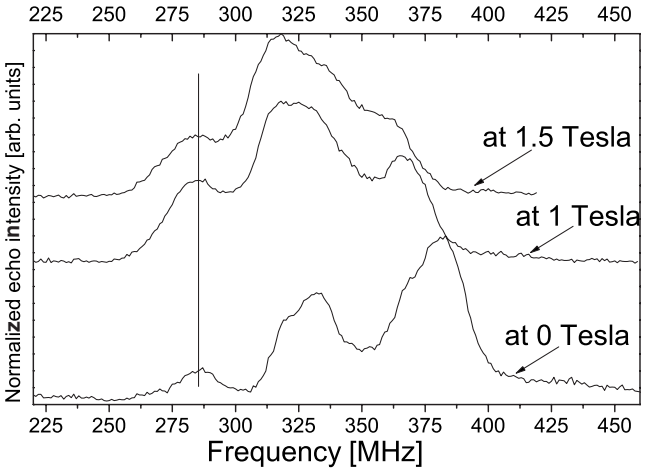


FIG. 4. The $^{55}$Mn NMR spin-echo spectra at 4.2 K for $La_{0.76}Sr_{2.24}Mn_2O_7$ ($x=0.62$) compound at field 0, 1, and 1.5 T. The vertical line at 285 MHz is to show that the $Mn^{4+}$ AFI line does not shift in the applied field. Line intensities are not corrected for differences in $\eta$.

$^{55}$Mn gyromagnetic ratio 10.55 MHz/T (the observed drop of 11 MHz corresponds to a decrease in the local field by 1.05 T). The $Mn^{4+}$ FMI line also shifts to lower frequencies in the applied field, but due to its overlap with other lines one cannot determine its exact shift in applied field.

Additional proof of the type of the magnetic order comes from a comparison of NMR enhancement factors $\eta$. For example, in the case of the $x=0.62$ compound the pulses which were used for the AFI line at 284 MHz were five times longer with ten times larger amplitude than pulses optimal for the FM DE line. This means that $\eta_{AFI}$ is at least 50 times smaller than $\eta_{FMM}$. The enhancement factor of the FMI line, $\eta_{FMI}$, is found to be six times smaller than $\eta_{FMM}$.

One has to keep in mind that the enhancement factor in the FM material is also much smaller for nuclei in domains than for nuclei in domain walls. However the possibility that the signal at 280–290 MHz comes from nuclei in FM ordered domains (smaller $\eta$) can be excluded as in the applied field such a line should also shift toward lower frequencies, which is not the case for $x=0.62$ compound.

In Fig. 3 also the spectra for the $x=0.68$ compound are presented and three lines are observed, corresponding to the AFI, FMI, and FMM. The neutron powder diffraction showed that for this doping level there is no magnetic LRO.[1] However, the muon spin rotation study by Coldea *et al.*[39] revealed that in the $x=0.68$ compound at low temperatures short-range magnetic order exists. Our NMR results support this finding and, furthermore, they indicate that the AF and two different in electronic properties FM regions (insulating or metallic) coexist. The width of the FMI $Mn^{4+}$ line for the $x=0.68$ compound is larger than for lower Sr-doped compounds ($x=0.5$ and 0.62) and amounts to 37 MHz. The linewidths in the case of $x=0.5$ and $x=0.62$ compounds amount to 22 and 26 MHz, respectively. This difference is attributed to a larger distribution of the static local magnetic fields in the $x=0.68$ compound with no LRO. This result is also consistent with that of muon spin rotation measurements.[39]

We were unable to detect the AFI signal in the compound with $x=0.5$ despite attempts with excitation conditions simi-

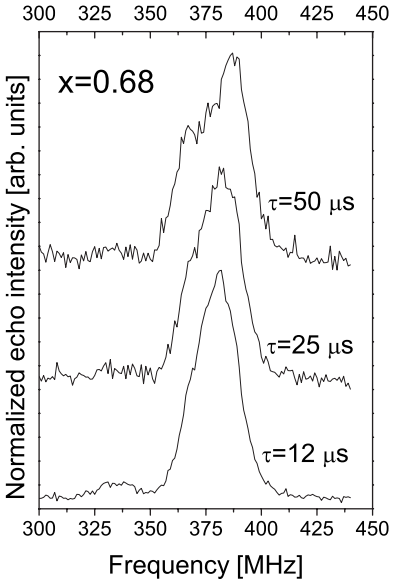


FIG. 5. The $^{55}$Mn NMR spin-echo spectra at 4.2 K of $La_{0.64}Sr_{2.36}Mn_2O_7$ ($x$=0.68) in zero applied field and pulse spacing $\tau$=12 $\mu$s, 25 $\mu$s, and 50 $\mu$s.

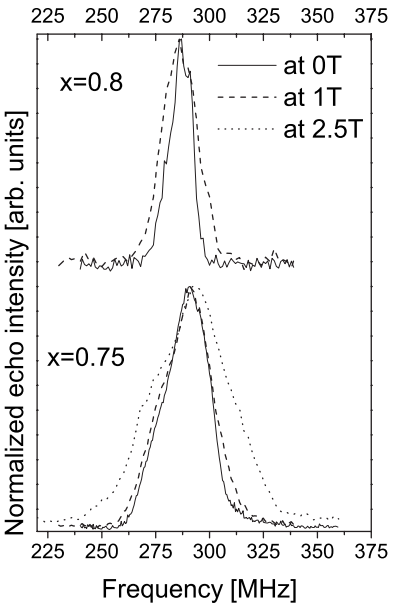


FIG. 6. The $^{55}$Mn NMR spin-echo spectra at 4.2 K of $La_{0.5}Sr_{2.5}Mn_2O_7$ ($x$=0.75) at 0 T (solid line), 1 T (dashed line), and 2.5 T (dotted line), and of $La_{0.4}Sr_{2.6}Mn_2O_7$ ($x$=0.8) at 0 T (solid line) and 1 T (dashed line).

lar to those for AFI signals in compounds with higher Sr content. Possible reasons of this fact are (a) the amount of the AFI phase decreases with decreasing Sr content, i.e., it is the lowest for $x$=0.5 compound, (b) the spin-spin relaxation time, $T_2$, of the AFI line decreases with decreasing Sr doping (see Table II) and is presumably the lowest for $x$=0.5 compound (for $x$=0.62 compound due to fast spin-spin relaxation we already "loose" 60% of the signal measured at the pulse spacing of 12 $\mu$s compared to 0 $\mu$s), and (c) $\eta$ of the AFI line for the $x$=0.5 compound may be even smaller than in the case of higher Sr-doped compounds.

In order to be able to say more about the size of the FMM regions (due to the DE interaction) in $La_{0.64}Sr_{2.36}Mn_2O_7$ ($x$=0.68) compound, three frequency-swept spectra with different value of pulse spacing were measured (Fig. 5). Unlike in the ferromagnetic metallic Sr-doped pseudocubic perovskites,[40,41] there is no clear minimum at the center of the DE line in the spectra measured with large pulse spacing. The absence of such minimum indicates that regions where DE interaction is effective are smaller than the range of the Suhl-Nakamura interaction,[42] which was found to be of 35 Å at 77 K for $La_{0.7}Sr_{0.3}MnO_3$.[40] Additionally, the intensity of FMI $Mn^{4+}$ line decreases faster than the DE line with increasing pulse spacing, which is due to a faster transverse nuclear relaxation of the $Mn^{4+}$ ions (see also Table II).

### B. NMR spectra in $La_{2-2x}Sr_{1+2x}Mn_2O_7$, $x$=0.75, and 0.8

The $^{55}$Mn NMR spectra of $La_{0.5}Sr_{2.5}Mn_2O_7$ ($x$=0.75) and $La_{0.4}Sr_{2.6}Mn_2O_7$ ($x$=0.8) at 0 T and in the applied field 1 and 2.5 T measured at 4.2 K are presented in Fig. 6. For both compounds only a single line centered at 290 and 287 MHz for the $x$=0.75 and $x$=0.8 compound, respectively, is observed in zero applied field. In the applied field also a single line is observed, and a lack of its shift indicates that this line is due to $Mn^{4+}$ in AF regions (see Table I). The absence of any signal from FM phases clearly indicates that such regions do not exist in these two compounds or their population/sizes are too small to be observed even by so sensitive method as NMR. This result is in contrast to pseudocubic AF ordered perovskite with a similar 2+ cation doping level, e.g., $La_{0.25}Ca_{0.75}MnO_3$ in which the FM DE line was observed at 4.2 K.[28]

The enhancement factor of the $Mn^{4+}$ AFI line for the $x$=0.75 and $x$=0.8 compounds is smaller than for $x$=0.62 and $x$=0.68. Even with the first pulse of the spin-echo sequence 10 $\mu$s long and maximum power of the 300 W pulse amplifier, we were unable to achieve the optimal excitation conditions for the $x$=0.75 and $x$=0.8 compounds. The necessity for using very long pulses at the full power clearly shows that the enhancement factor, $\eta$, for $x$=0.75 and $x$=0.8 compounds is smaller that in the case of the AFI line for $x$=0.62 and $x$=0.68 compounds. This indicates a more "perfect" AF order or/and a higher magnetocrystalline anisotropy in the former compounds. Indeed, this is consistent with the magnetic structures determined by the neutron diffraction.[1] The compound with $x$=0.62 has FM ordered planes coupled AF (four Mn neighbors FM coupled and two AF coupled), while $x$=0.75 and $x$=0.8 compounds have FM ordered "rods" (two neighbors coupled FM and four AF coupled) (see Fig. 1). Both, the small $\eta$ and a lack of shift of the resonance line in the applied field prove that the observed signal comes from AF ordered regions, similarly to the $x$=0.62 and $x$=0.68 compounds. As was already mentioned also $M$ versus $H$ curves did not show any ferromagnetic contribution (Fig. 2).

We failed to detect any NMR spin-echo signal from the $x$=1 compound (all Mn nearest-neighbor coupled AF). Attempts in the frequency range 200–350 MHz with excitation conditions similar to those used in the case of $x$=0.75 and

TABLE I. Results of the Gaussian curve fits to the frequency-swept spectra (see Fig. 6): the linewidth and central frequency for $x=0.75$ and $x=0.8$ compounds at 4.2 K.

| | | | 0 T | 1 T | 2.5 T |
|---|---|---|---|---|---|
| | Linewidth | MHz | 21.1 | 24.5 | 36.5 |
| $x=0.75$ | Central frequency | MHz | 289.6 | 289.7 | 291.9 |
| | Linewidth | MHz | 10.9 | 16.3 | |
| $x=0.8$ | Central frequency | MHz | 286.7 | 286.2 | |

$x=0.8$ compounds both in zero applied field and at 1 T did not provide any measurable spin-echo signal.

### C. Spin-spin relaxation rates

For all the studied compounds measurements of the spin-spin relaxation time $T_2$ were carried out by varying the pulse spacing $\tau$ in the two pulse spin-echo sequence. The results of the spin-echo decay measurements are presented in Table II. A single exponential decay was assumed and the following formula was used to fit the data:

$$A(\tau) = A_n + A_{\tau=0} \exp\left(-\frac{2\tau}{T_2}\right), \tag{3}$$

where $A(\tau)$ and $A_{\tau=0}$ are the spin-echo amplitudes at the pulse separation $\tau$ and $\tau=0$, respectively, and $A_n$ parameter corresponds to the noise level.

Table II presents spin-spin relaxation times obtained for all the observed resonant lines. The nuclear spin-spin relaxation in FMM regions with the DE interaction effective is due to fluctuations of the hyperfine fields related to the fast hopping of the electron holes.[43] The nuclear spin-spin relaxation time of the FMI $Mn^{4+}$ ions is shorter than that of the DE line. In the case of FMI regions the mechanism of the spin-spin relaxation is different than in the case of the FMM regions and is assigned to fluctuations of the magnetic hyperfine field and the electric-field gradient (EFG) related to the motion of the Jahn-Teller polarons.[44] According to the model proposed by Savosta *et al.*[44] the charge carriers in the FMI regions can be regarded as the small Jahn-Teller polarons, and their movement is accompanied by a lattice excitation leading to a fluctuation of the EFG. The $T_2$ of nuclei in the FMI regions was found to be shorter than $T_2$ of nuclei in the FMM state in several pseudocubic perovskite manganites, for example, in $La_{1-\delta}MnO_3$ (Ref. 44) or $La_{0.9}Ca_{0.1}MnO_3$.[45]

The spin-spin relaxation times of the AFI lines are longer than for nuclei in the FM regions (see Table II). For $x=0.75$ and $x=0.8$ compounds $T_2$ in AFI regions is twice longer than $T_2$ in FM regions (insulating or metallic) in the $x=0.5$, $x=0.62$, and $x=0.68$ compounds. For the $x=0.75$ compound measurements of $T_2$ in the applied field were also carried out (see Table II). The results indicate that $T_2$ increases by 20% at 2.5 T compared to $T_2$ at 0 T, which can be partly attributed to the field dependence of $T_2$ resulting from the Suhl-Nakamura interaction, due to which $T_2$ increases as the external field increases.[46,47] Such effect was also observed in the manganese ferrite[48] and in $La_{0.69}Pb_{0.31}MnO_3$.[49]

TABLE II. Values of the spin-spin relaxation times $T_2$ and their uncertainties, $\Delta T_2$, determined at 4.2 K for the AFI $Mn^{4+}$ line (at the frequencies of 290 MHz), FMI $Mn^{4+}$ line (330 MHz), and the FM DE line (at the frequencies of 380 MHz).

| | Frequency (MHz) | $T_2$ ($\mu$s) | $\Delta T_2$ ($\mu$s) |
|---|---|---|---|
| $x=0.5$ | 330 (FMI) | 20.1 | 0.3 |
| | 375 (FMM) | 24.2 | 0.6 |
| $x=0.62$ | 286 (AFI) | 29.4 | 1.9 |
| | 330 (FMI) | 24.0 | 0.6 |
| | 380 (FMM) | 33.3 | 1.1 |
| $x=0.68$ | 290 (AFI) | 40.9 | 1.4 |
| | 380 (FMM) | 30.6 | 1.1 |
| $x=0.75$ | 290 (AFI at 0 T) | 58.6 | 0.8 |
| | 290 (at 1 T) | 62.2 | 1.3 |
| | 290 (at 2.5 T) | 69.9 | 1.9 |
| $x=0.8$ | 288 (AFI at 0 T) | 56.8 | 3.2 |

## III. CONCLUSIONS

The $^{55}Mn$ NMR has been used as a local probe of the magnetic arrangement in highly doped bilayered manganese perovskites $La_{2-2x}Sr_{1+2x}Mn_2O_7$. The study has shown unambiguously that the compounds $x=0.5$ and 0.62, both of the $A$-type AFI order ($T_N \sim 200$ K) according to previous neutron-diffraction work, are in fact phase separated. This is manifested by observation of NMR signals from $Mn^{4+}$ and $Mn^{3+}$ ions in the short-range ordered FMI, as well as FMM regions in addition to the signal from $Mn^{4+}$ ions in the long-range ordered AFI phase. The coexistence of these three phases has been detected also in the $x=0.68$ compound with no long-range magnetic order. The amount of the FMI and FMM phases relative to the AFI one has been found to decrease with Sr doping, and no FM signals have been detected for higher Sr-doped compounds $x=0.75$ and $x=0.8$ with the $C$ or $C^*$-type AF order ($T_N \sim 200$ K) and for $x=1$ with the $G$-type order ($T_N=160$ K). The lack of FM behavior in these samples, confirmed also by magnetization measurements, points to a decreased strength of DE interaction (or itinerancy of electrons) in the bilayered (two-dimensional)

perovskites compared to the pseudocubic (three-dimensional) systems such as $La_{1-x}Ca_xMnO_3$ or $Pr_{1-x}Ca_xMnO_3(x \to 1)$, where the FM phase is stabilized in addition to the *G*-type one.[34,50,51] It should be noted, however, that such FM phase is not formed in analogous three-dimensional system $Pr_{1-x}Sr_xMnO_3$. In that case, the itinerancy seems to be hindered by extrinsic tetragonal distortion of the *G*-type phase due to its epitaxial stacking with coexisting *C*-type regions,[50] which has probably the same effect as the decreased dimensionality in the present bilayered perovskites $La_{2-2x}Sr_{1+2x}Mn_2O_7$.

## ACKNOWLEDGMENTS

Financial supports by the EU grant under Contract No. NMP4-CT-2005-517039 (CoMePhS), the Grant Agency of Czech Republic under Project No. 202/06/0051, and partial support of the Polish Ministry of Science and Higher Education are acknowledged.

[1] J. F. Mitchell, D. N. Argyriou, A. Berger, K. E. Gray, R. Osborn, and U. Welp, J. Phys. Chem. B **105**, 10731 (2001).
[2] M. Pissas and G. Kallias, Phys. Rev. B **68**, 134414 (2003).
[3] M. Pissas and G. Papavassiliou, J. Phys.: Condens. Matter **16**, 6527 (2004).
[4] M. Paraskevopoulos, F. Mayr, J. Hemberger, A. Loidl, R. Heichele, D. Maurer, V. ller, A. A. Mukhin, and A. M. Balbashov, J. Phys.: Condens. Matter **12**, 3993 (2000).
[5] E. O. Wollan and W. C. Koehler, Phys. Rev. **100**, 545 (1955).
[6] C. Zener, Phys. Rev. **82**, 403 (1951).
[7] P. W. Anderson and H. Hasegawa, Phys. Rev. **100**, 675 (1955).
[8] M. Uehara, S. Mori, C. H. Chen, and S. W. Cheong, Nature (London) **399**, 560 (1999).
[9] C. Renner, G. Aeppli, B. G. Kim, Y.-A. Soh, and S. W. Cheong, Nature (London) **416**, 518 (2002).
[10] J. C. Loudon, N. D. Mathur, and P. A. Midgley, Nature (London) **420**, 797 (2002).
[11] J. H. Yoo, Y. Murakami, D. Shindo, T. Atou, and M. Kikuchi, Phys. Rev. Lett. **93**, 047204 (2004).
[12] S. Yunoki, J. Hu, A. L. Malvezzi, A. Moreo, N. Furukawa, and E. Dagotto, Phys. Rev. Lett. **80**, 845 (1998).
[13] A. Moreo, S. Yunoki, and E. Dagotto, Science **283**, 2034 (1999).
[14] A. Moreo, M. Mayr, A. Feiguin, S. Yunoki, and E. Dagotto, Phys. Rev. Lett. **84**, 5568 (2000).
[15] E. Dagotto, *Nanoscale Phase Separation and Colossal Magnetoresistance* (Springer Verlag, Berlin, 2003).
[16] J. Burgy, A. Moreo, and E. Dagotto, Phys. Rev. Lett. **92**, 097202 (2004).
[17] D. Khomskii and L. Khomskii, Phys. Rev. B **67**, 052406 (2003).
[18] T. G. Perring, G. Aeppli, T. Kimura, Y. Tokura, and M. A. Adams, Phys. Rev. B **58**, R14693 (1998).
[19] M. Matsukawa, H. Ogasawara, R. Sato, M. Yoshizawa, R. Suryanarayanan, G. Dhalenne, A. Revcolevschi, and K. Itoh, Phys. Rev. B **62**, 5327 (2000).
[20] C. D. Ling, J. E. Millburn, J. F. Mitchell, D. N. Argyriou, J. Linton, and H. N. Bordallo, Phys. Rev. B **62**, 15096 (2000).
[21] J. F. Mitchell, J. E. Millburn, M. Medarde, S. Short, J. D. Jorgensen, and M. T. Fernandez-Diaz, J. Solid State Chem. **141**, 599 (1998).
[22] V. Likodimos and M. Pissas, Phys. Rev. B **76**, 024422 (2007).
[23] G. Allodi, R. De Renzi, G. Guidi, F. Licci, and M. W. Pieper, Phys. Rev. B **56**, 6036 (1997).
[24] G. Papavassiliou, M. Fardis, M. Belesi, M. Pissas, I. Panagiotopoulos, G. Kallias, D. Niarchos, C. Dimitropoulos, and J. Dolinsek, Phys. Rev. B **59**, 6390 (1999).
[25] G. Papavassiliou, M. Fardis, M. Belesi, T. G. Maris, G. Kallias, M. Pissas, D. Niarchos, C. Dimitropoulos, and J. Dolinsek, Phys. Rev. Lett. **84**, 761 (2000).
[26] J. P. Renard and A. Anane, Mater. Sci. Eng., B **63**, 22 (1999).
[27] C. Kapusta, P. C. Riedi, M. Sikora, and M. R. Ibarra, Phys. Rev. Lett. **84**, 4216 (2000).
[28] C. Kapusta, P. C. Riedi, W. Kocemba, M. R. Ibarra, and J. M. D. Coey, J. Appl. Phys. **87**, 7121 (2000).
[29] C. Kapusta, P. C. Riedi, D. Rybicki, C. J. Oates, D. Zajac, M. Sikora, C. Marquina, and M. R. Ibarra, J. Magn. Magn. Mater. **272-276**, 1759 (2004).
[30] K. Shimizu, W. Boujelben, and A. Cheikh-Rouhou, Phys. Status Solidi A **201**, 1421 (2004).
[31] J. Millburn, J. F. Mitchell, and D. N. Argyriou, Chem. Commun. (Cambridge) **1999**, 1389.
[32] A. M. Portis and A. C. Gossard, J. Appl. Phys. **31**, S205 (1960).
[33] G. Matsumoto, J. Phys. Soc. Jpn. **29**, 615 (1970).
[34] M. M. Savosta, P. Novák, M. Marysko, Z. Jirk, J. Hejtmánek, J. Englich, J. Kohout, C. Martin, and B. Raveau, Phys. Rev. B **62**, 9532 (2000).
[35] R. E. Watson and A. J. Freeman, Phys. Rev. **123**, 2027 (1961).
[36] G. Allodi, R. De Renzi, F. Licci, and M. W. Pieper, Phys. Rev. Lett. **81**, 4736 (1998).
[37] S. D. Bader, R. M. Osgood Iii, D. J. Miller, J. F. Mitchell, and J. S. Jiang, J. Appl. Phys. **83**, 6385 (1998).
[38] J. Sloan, P. D. Battle, M. A. Green, M. J. Rosseinsky, and J. F. Vente, J. Solid State Chem. **138**, 135 (1998).
[39] A. I. Coldea, S. J. Blundell, C. A. Steer, J. F. Mitchell, and F. L. Pratt, Phys. Rev. Lett. **89**, 277601 (2002).
[40] M. M. Savosta and P. Novák, Phys. Rev. Lett. **87**, 137204 (2001).
[41] D. Rybicki, M. Sikora, C. Kapusta, P. C. Riedi, Z. Jirak, K. Knizek, M. Marysko, E. Pollert, and P. Veverka, Phys. Status Solidi C **3**, 155 (2006).
[42] H. Suhl, Phys. Rev. **109**, 606 (1958).
[43] M. M. Savosta, V. A. Borodin, and P. Novák, Phys. Rev. B **59**, 8778 (1999).
[44] M. M. Savosta, V. I. Kamenev, V. A. Borodin, P. Novák, M. Marysko, J. Hejtmánek, K. Dörr, and M. Sahana, Phys. Rev. B **67**, 094403 (2003).
[45] P. A. Algarabel, J. M. De Teresa, J. Blasco, M. R. Ibarra, C. Kapusta, M. Sikora, D. Zajac, P. C. Riedi, and C. Ritter, Phys. Rev. B **67**, 134402 (2003).
[46] D. Hone, V. Jaccarino, T. Ngwe, and P. Pincus, Phys. Rev. **186**, 291 (1969).

[47] J. H. Davis and C. W. Searle, Phys. Rev. B **9**, 323 (1974).
[48] J. H. Davis and C. W. Searle, Phys. Rev. B **14**, 2126 (1976).
[49] L. K. Leung and A. H. Morrish, Phys. Rev. B **15**, 2485 (1977).
[50] C. Martin, A. Maignan, M. Hervieu, B. Raveau, Z. Jirak, M. M. Savosta, A. Kurbakov, V. Trounov, G. Andre, and F. Bouree, Phys. Rev. B **62**, 6442 (2000).
[51] C. D. Ling, E. Granado, J. J. Neumeier, J. W. Lynn, and D. N. Argyriou, J. Magn. Magn. Mater. **272-276**, 246 (2004).